

An Improved Voltage Controller for Distribution Static Compensator

Sanath Saralaya*[‡], K Manjunatha Sharma**

*Department of Electrical and Electronics, Research scholar, National Institute of Technology Karnataka, Surathkal, India

**Department of Electrical and Electronics, Associate Professor, National Institute of Technology Karnataka, Surathkal, India

(sanathsaralaya@gmail.com, manjunatha.sharma@gmail.com)

[‡]Corresponding Author; Sanath Saralaya, Department of Electrical and Electronics, Research scholar, National Institute of Technology Karnataka, Surathkal, India, sanathsaralaya@gmail.com

Received: 08.11.2018 Accepted: 11.01.2019

Abstract- Distribution System consist of different types of loads like linear and nonlinear load. Due to different types of loads, voltage unbalance and other power quality related issues will occur. To overcome this problem, a voltage source inverter based device called distribution static compensator can be used. In this work, an improved voltage controller for distributed static compensator, based on power balancing theory is presented. The improved controller uses only voltage sensors and this controller is developed by considering unbalanced load conditions. Proportional Integral controller is used for maintaining terminal voltage and DC link voltage. The controller is verified for different voltage disturbances such as sag and swell. MATLAB/SIMULINK package is used to verify the controller using simulation. The controller is also verified using Hardware in the loop simulation using DSPICE and results are presented for different voltage disturbances.

Keywords: Hardware in the loop simulation; PI Controller; Voltage sag; Voltage swell; Voltage source Converter.

1. Introduction

The power system is divided into three parts, which are generation, transmission and distribution. In the power system, the distribution network is considered as the weakest part because the major portion of power loss takes place in this section. The distribution system has low voltage profiles and various types of faults and radial structure, which will affect the reliability of the distribution network. Compared to transmission network, distribution network has greater R/X ratio due to which problems such as voltage instability and high power loss arise. It is estimated that the I^2R loss in the distribution network is 13% of the total power generated [1]. Most of the loads in modern distribution network are inductive and nonlinear loads. Therefore, the system will have lagging power factor and this will result in the reduction in the voltage profile, increase in loss and increase in harmonics.

Traditionally the voltage is maintained by connecting the shunt capacitors to the distribution network. The major limitation of shunt capacitor is that they cannot generate the consistent variable reactive power. Because of this limitation, the idea of FACTS devices is evolved. FACTS devices are typically used in the transmission line. FACTS devices in the distribution network are termed as custom power devices

(CPD) [2]. Distributed Static Compensator (DSTATCOM) is one of the shunt connected voltage source converter (VSC) based CPD.

DSTATCOM perform a noteworthy part in voltage balancing, improving voltage profile and lowering power losses in the system, under dynamic and steady state conditions. The optimal performance of DSTATCOM depends on the control algorithm used. In literature, many topologies and control algorithms are proposed [3-5]. An improved current control algorithm is proposed using the self-tuned filter in DSTATCOM based on instantaneous reactive power theory for the extraction of fundamental component of load currents and reduce the switching ripples [6]. In literature, the proportional integral controller is used as controller. But the tuning problem must be resolved satisfactorily. To overcome this issue, a fuzzy PI controller based algorithm is used in DSTATCOM to maintain the voltage stability in distribution network [7]. The control algorithms are also proposed based on intelligent computation methods such as learning vector quantization, leaky least mean square, back propagation algorithms, etc. to enhance the power quality [8-12]. The different topologies are presented for four wire and three wire networks and aim to reduce the dc link rating. Supply of both reactive and real power from DSTATCOM is achieved by connecting active

source to the VSC [13], [14]. A hybrid particle swarm optimisation – firefly algorithm based controller is proposed to enhance the power quality in wind power distribution system [15]. A study on the performance of DSTATCOM on power quality issues with the presence of wind energy is analysed. In this case, a DSTATCOM with battery is used with synchronous reference frame (SRF) based control algorithm [16]. The selection of topology and reference algorithms are mainly dependant on the system requirement.

In many works, current control algorithms are presented. But very less work is done on voltage control mode algorithms [17], [18]. The current sensorless voltage controllers based on power balancing theory are proposed in [19]. In this, the authors considered only balanced voltage condition and have not tested for unbalanced and nonlinear load conditions. In this paper, an improved current sensorless voltage controller is presented for unbalanced load conditions. The improved controller is developed using power balancing theory using the synchronous reference frame. The presented controller is simulated in MATLAB and also verified using hardware in the loop simulation using DSPACE. The organization of this paper is done in the following way. Section 2 gives the details about the controller. Section 3 provides results of simulation and hardware in loop simulations and in section 4 conclusion is given.

2. Control Algorithm

A power balanced theory based improved voltage control algorithm is presented. The DSTATCOM is in parallel with the load, which consists of a filter and the VSC. L_s and R_s represent the line impedance. The regulation of voltage at the point of common coupling (PCC) is DSTATCOMs main function.

In steady state condition, real and reactive power of three phase system in terms of SRF quantities are as shown in equation (1) and (2). (v_d, v_q, v_0) and (i_d, i_q, i_0) are the SRF components of voltage and current respectively. P and Q are real and imaginary power respectively.

$$P = \frac{3}{2}(v_d i_d + v_q i_q + 2v_0 i_0) \tag{1}$$

$$Q = \frac{3}{2}(v_d i_q - v_q i_d) \tag{2}$$

The total power supplied from the VSC is equal to the sum of the power delivered to the PCC and the loss in the filter components. The power flow from VSC to the PCC is shown in fig. 1. The total power is given eq. (3), where S_e, S_o and S_f are the power from VSC, power at PCC and loss in the filter respectively.

$$S_e = S_o + S_f \tag{3}$$

$$P_e + jQ_e = (P_o + jQ_o) + (P_f + jQ_f) \tag{4}$$

$$P_e = P_o + P_f \tag{5}$$

$$Q_e = Q_o + Q_f \tag{6}$$

The delivered power to the PCC and output power of VSC in SRF are written as shown in eq (7), (8), (9) and (10).

$$P_o = \frac{3}{2}(v_d i_d + v_q i_q + 2v_0 i_0) \tag{7}$$

$$Q_o = \frac{3}{2}(v_d i_q - v_q i_d) \tag{8}$$

$$P_e = \frac{3}{2}(e_d i_d + e_q i_q + 2e_0 i_0) \tag{9}$$

$$Q_e = \frac{3}{2}(e_d i_q - e_q i_d) \tag{10}$$

The loss in power at the filter components are given by

$$P_f = \frac{3}{2}(i_d^2 + i_q^2)R_f \tag{11}$$

$$Q_f = \frac{3}{2}(i_d^2 + i_q^2)\omega L_f \tag{12}$$

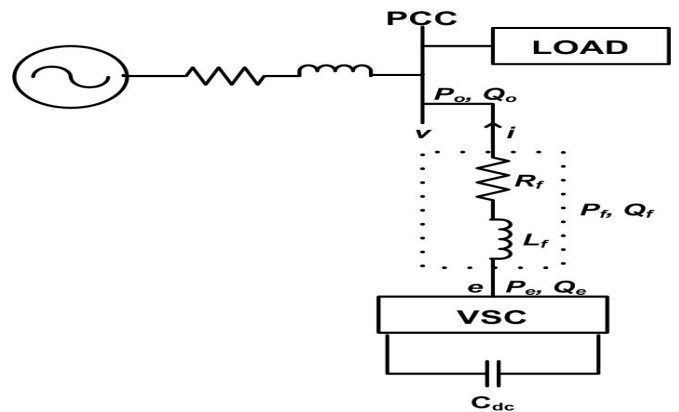


Fig. 1. Single line diagram

Substituting (7), (9) and (11) in (5) and (8), (10) and (12) in (6) yields

$$\frac{3}{2}(e_q i_q + e_d i_d + 2e_0 i_0) = \frac{3}{2}(i_d^2 + i_q^2)R_f + \frac{3}{2}(2v_0 i_0 + v_d i_d + v_q i_q) \tag{13}$$

$$\frac{3}{2}(e_q i_d - e_d i_q) = \frac{3}{2}(i_d^2 + i_q^2)\omega L_f + \frac{3}{2}(v_q i_d - v_d i_q) \tag{14}$$

It is assumed that the 0th component generated from VSC

is equal to the actual 0th component of PCC, i.e. $e_0=v_0$. Therefore, from Eq. (13) and (14) yields

$$e_d = (R_f i_d - \omega L_f i_q) + v_d \tag{15}$$

$$e_q = (R_f i_q + \omega L_f i_d) + v_q \tag{16}$$

e_d and e_q are obtained from i_d , i_q , R_f and L_f as shown in equations (15) and (16). Fig. 2 shows the block diagram of the presented control strategy for DSTATCOM. As shown in the figure, three phase to dq0 transformation is done using eq. (17).

$$\begin{bmatrix} v_0 \\ v_d \\ v_q \end{bmatrix} = \sqrt{\frac{2}{3}} \begin{bmatrix} \frac{1}{\sqrt{2}} & \frac{1}{\sqrt{2}} & \frac{1}{\sqrt{2}} \\ \cos \theta & \cos \left(\theta - \frac{2\pi}{3} \right) & \cos \left(\theta + \frac{2\pi}{3} \right) \\ \sin \theta & \sin \left(\theta - \frac{2\pi}{3} \right) & \sin \left(\theta + \frac{2\pi}{3} \right) \end{bmatrix} \begin{bmatrix} v_a \\ v_b \\ v_c \end{bmatrix} \tag{17}$$

From fig.2., it is observed that the regulation of DC link voltage is done by the PI controller, and the output of which is taken as i_d , as shown in Eq. (18). Similarly, i_q is obtained from the PI controller which regulates the PCC voltage, given in Eq. (19).

$$i_d = \left(k_{pdc} + \frac{k_{idc}}{s} \right) (V_{dc}^* - V_{dc}) \tag{18}$$

$$i_q = \left(k_{pac} + \frac{k_{iac}}{s} \right) (V_{pcc}^* - V_{pcc}) \tag{19}$$

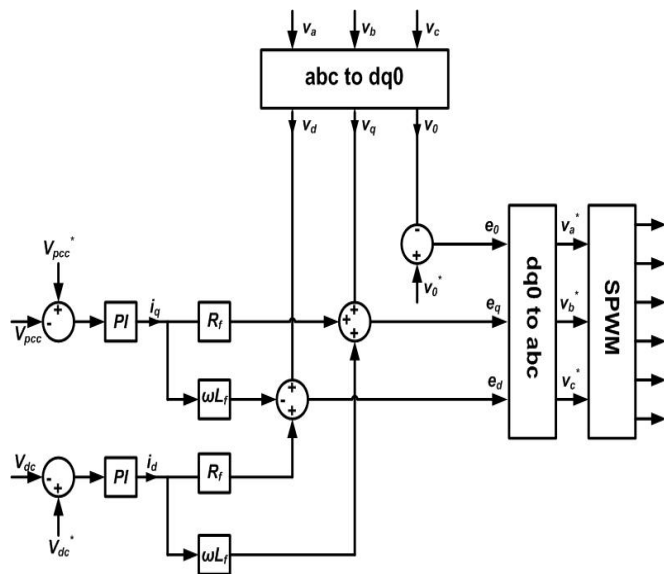


Fig. 2. Control Strategy of DSTATCOM

Where k_{pdc} and k_{idc} are the PI controller gains which are used to control the DC link voltage. Similarly, k_{pac} and k_{iac} are the PI controller gains which used to regulate the PCC voltage. Substituting Eq. (18) and (19) in Eq. (15) and (16),

$$e_d = \left(k_{pdc} + \frac{k_{idc}}{s} \right) (V_{dc}^* - V_{dc}) R_f - \omega L_f \left(k_{pac} + \frac{k_{iac}}{s} \right) (V_{pcc}^* - V_{pcc}) + v_d \tag{20}$$

$$e_q = \left(k_{pac} + \frac{k_{iac}}{s} \right) (V_{pcc}^* - V_{pcc}) R_f + \omega L_f \left(k_{pdc} + \frac{k_{idc}}{s} \right) (V_{dc}^* - V_{dc}) + v_q \tag{21}$$

$$e_0 = v_0^* - v_0 \tag{22}$$

The reference value of output voltage of the inverter is obtained using transformation, which is shown in Eq. (23).

$$\begin{bmatrix} v_a^* \\ v_b^* \\ v_c^* \end{bmatrix} = \sqrt{\frac{2}{3}} \begin{bmatrix} \frac{1}{\sqrt{2}} & \cos \theta & \sin \theta \\ \frac{1}{\sqrt{2}} & \cos \left(\theta - \frac{2\pi}{3} \right) & \sin \left(\theta - \frac{2\pi}{3} \right) \\ \frac{1}{\sqrt{2}} & \cos \left(\theta + \frac{2\pi}{3} \right) & \sin \left(\theta + \frac{2\pi}{3} \right) \end{bmatrix} \begin{bmatrix} e_0 \\ e_d \\ e_q \end{bmatrix} \tag{23}$$

The modified control algorithm is derived by considering the unbalanced condition. The modified controller is simulated for different operating conditions of the distribution system. The simulation results and hardware in the loop simulation results are presented in the following section for different voltage disturbances.

3. Simulation Results

In this section simulation and hardware in the loop results are presented. Details of the system considered for simulation is given in the appendix. The system consists of the nonlinear and unbalanced load. The nonlinear load is a three phase rectifier with RL load. For simulation MATLAB Simulink is used. Hardware in the loop simulation is a virtual real time simulation where the real version of controller and virtual plant model is considered for verification. In this section, hardware in the loop simulation results are also presented. Table 1 presents the different cases considered for the simulations and hardware in the loop simulations.

3.1. Case I:

In this case, the system with the unbalanced and nonlinear load without DSTATCOM is simulated and results are presented. Fig 3 shows the pu voltage (RMS) at the PCC. The voltage at PCC is 0.92 pu. Instantaneous voltage waveform is shown in fig. 4, and it is observed that waveform is distorted because of the nonlinear load. Fig 5

shows three phase voltage waveform and the pu value of the voltage at PCC obtained in hardware in loop simulation.

Table 1. Different cases for simulations

Case No.	Details
I	Without DSTATCOM with the unbalanced and nonlinear load.
II	With DSTATCOM with the unbalanced and nonlinear load.
III	With sag and without DSTATCOM
IV	With sag and with DSTATCOM
V	With swell and without DSTATCOM
VI	With swell and with DSTATCOM

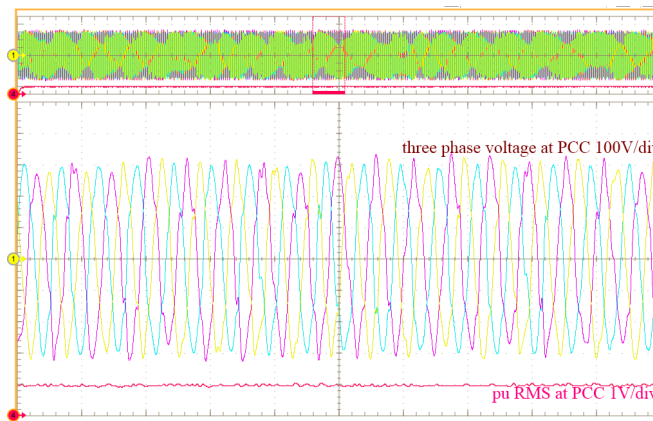


Fig. 5. RMS voltage and Instantaneous voltage at PCC without DSTATCOM (Hardware in-loop)

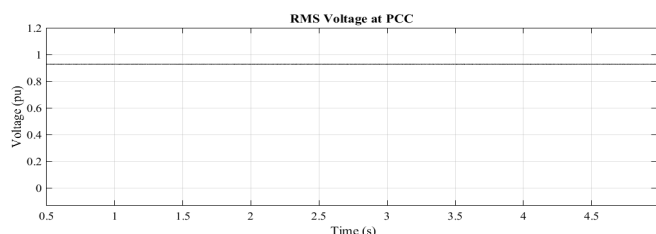


Fig. 3. RMS voltage at PCC without DSTATCOM (MATLAB Simulation)

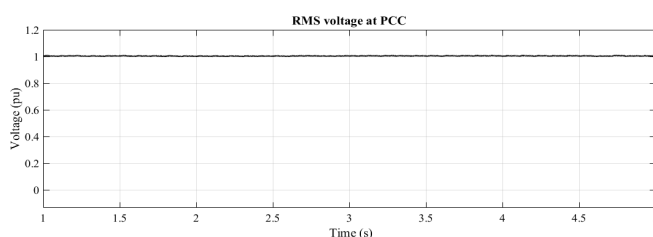


Fig. 6. RMS voltage at PCC with DSTATCOM (MATLAB Simulation)

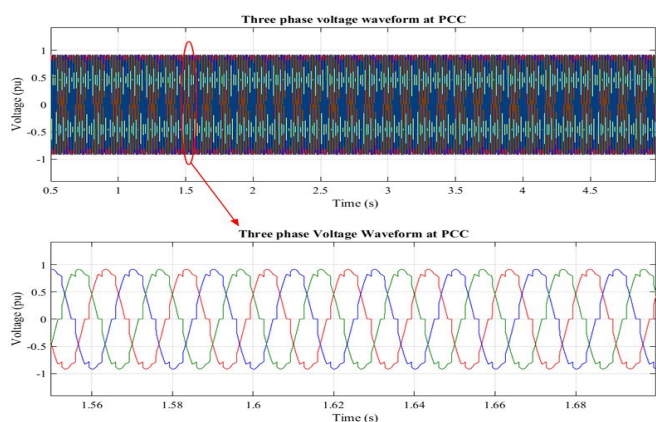


Fig. 4. Instantaneous voltage at PCC without DSTATCOM (MATLAB Simulation)

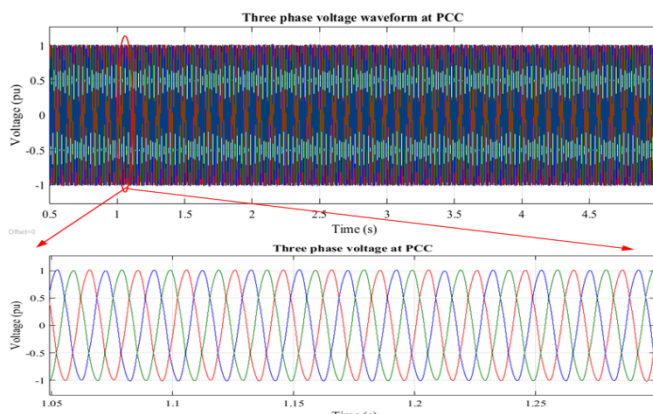


Fig. 7. Instantaneous voltage at PCC with DSTATCOM (MATLAB Simulation)

3.2. Case II:

In this case, the results are observed by connecting the DSTATCOM. Fig 6 shows the RMS value of the voltage at PCC which is maintained at 1 pu after connecting the DSTATCOM. After connecting DSTATCOM the voltage at PCC becomes pure sinusoidal and voltage is balanced, which is shown in fig 7. The reactive power supplied from DSTATCOM is shown in fig 8. Fig 9 shows the results of hardware in the loop simulation. From the results, its observed that the voltage is balanced and regulated at reference value.

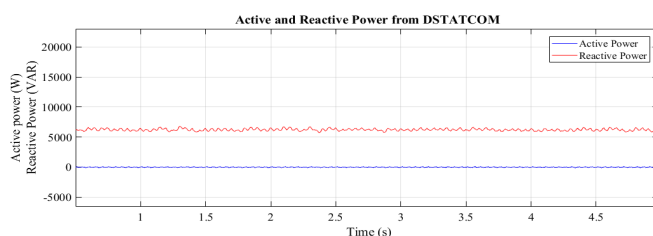


Fig. 8. Reactive and active power supplied from DSTATCOM (MATLAB Simulation)

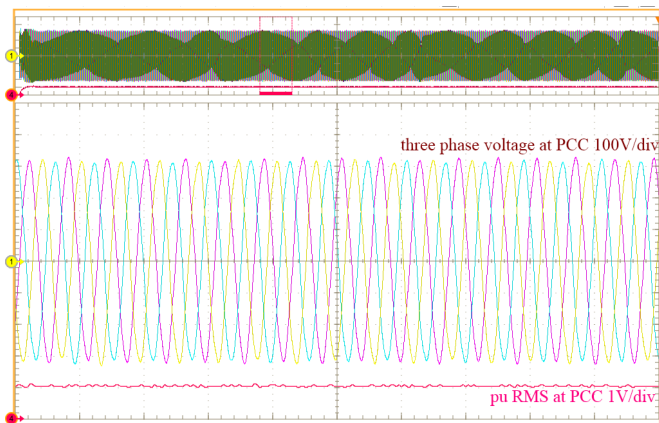


Fig. 9. RMS voltage and Instantaneous voltage at PCC with DSTATCOM (Hardware in-loop)

3.3. Case III:

In this case, the resistive load of 10Ω at each phase is switched on at 2 s to create voltage sag and it is cleared at 3 s. At the time of sag, RMS voltage is reduced to 0.82 pu, as shown in fig 10. Fig 11 shows the voltage waveform at PCC in the absence of DSTATCOM. Similar results are observed in hardware in loop simulation also, which is shown in fig 12.

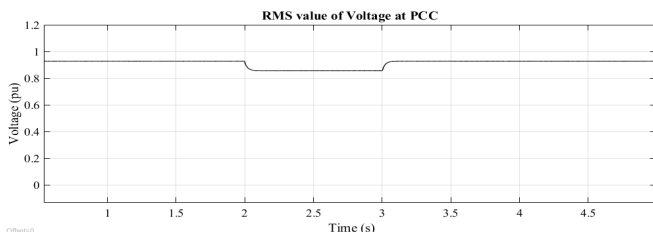


Fig. 10. RMS voltage at PCC without DSTATCOM with sag (MATLAB Simulation)

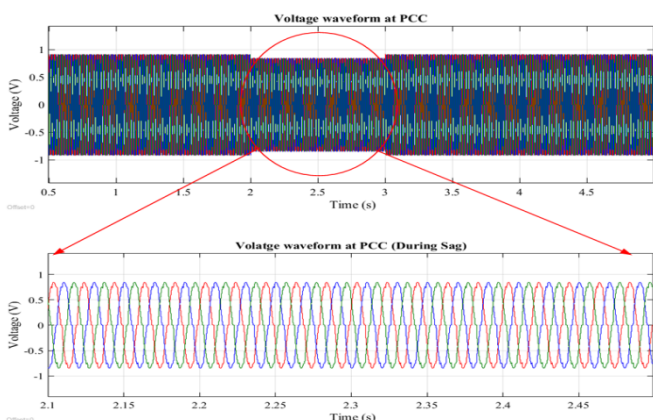


Fig. 11. Instantaneous voltage at PCC without DSTATCOM (MATLAB Simulation)

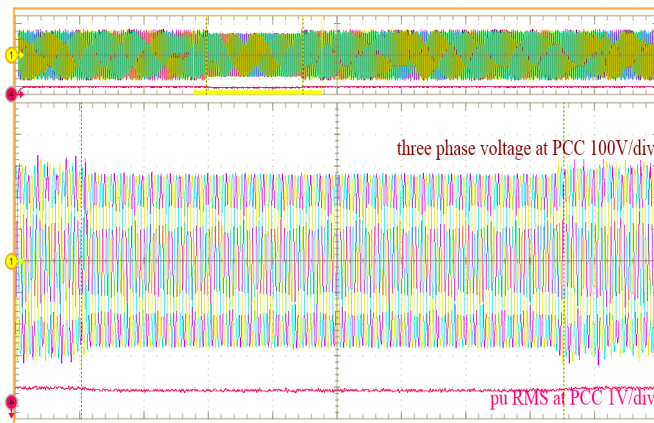


Fig. 12. RMS voltage and Instantaneous voltage at PCC with sag without DSTATCOM (Hardware in-loop)

3.4. Case IV:

In this case, sag is created at 2 s and it is cleared at 3 s, but in this case DSTATCOM is connected. When sag occurs at 2 s, the controller takes 0.2 s time to settle and maintain the voltage at 1 pu. Similarly, when sag is cleared, the controller takes time of 0.2 s and maintains the voltage at 1pu, which is observed from PCC voltage waveform shown in fig 13. Fig 14 shows the RMS voltage at PCC and power supplied from DSTATCOM. From fig 14 it is observed that, during the sag the reactive power supplied from DSTATCOM is increased such that voltage is maintained at 1 pu. Fig 15 and 16 shows the three phase voltage waveform during starting of the sag and end of the sag respectively.

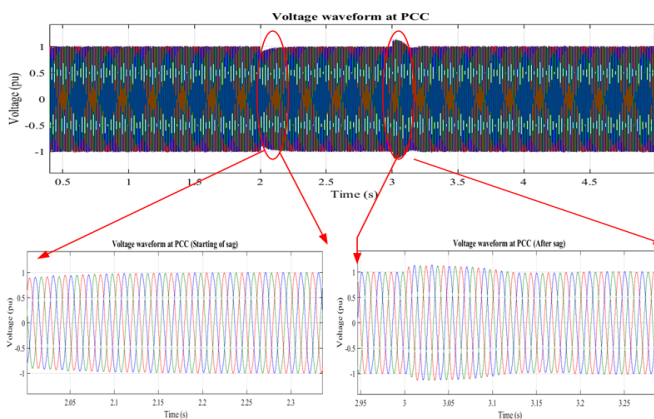


Fig. 13. Instantaneous voltage at PCC with DSTATCOM and with sag (MATLAB Simulation)

3.5. Case V:

In this case, swell is created by switching off the large resistive load at 2 s for the duration of 1 s. In this case DSTATCOM is absent. Fig 17 shows the RMS voltage at PCC. Fig 18 and 19 show the instantaneous voltage waveform in MATLAB simulation and Hardware in loop simulations.

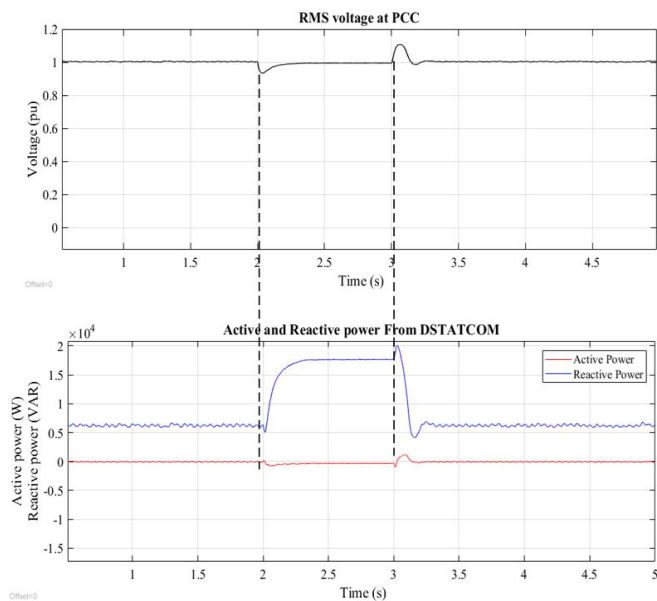


Fig. 14. RMS voltage at PCC and power supplied from DSTATCOM with sag (MATLAB Simulation)

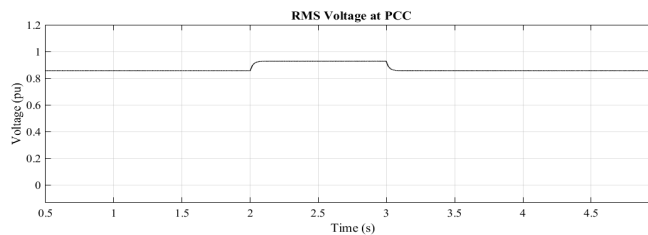


Fig. 17. RMS voltage at PCC without DSTATCOM with swell (MATLAB Simulation)

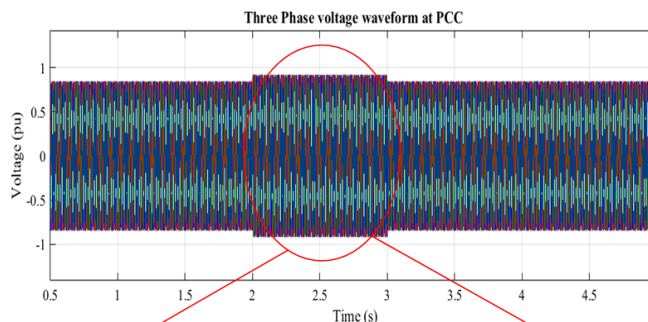


Fig. 18. Instantaneous voltage at PCC without DSTATCOM with swell (MATLAB Simulation)

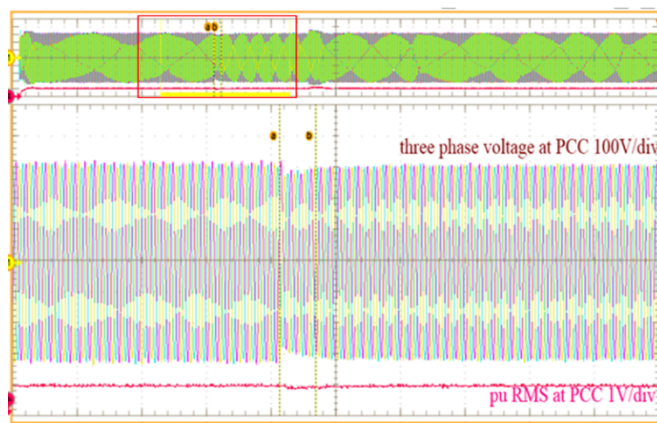


Fig. 15. RMS voltage and Instantaneous voltage at PCC starting of sag with DSTATCOM (Hardware in-loop)

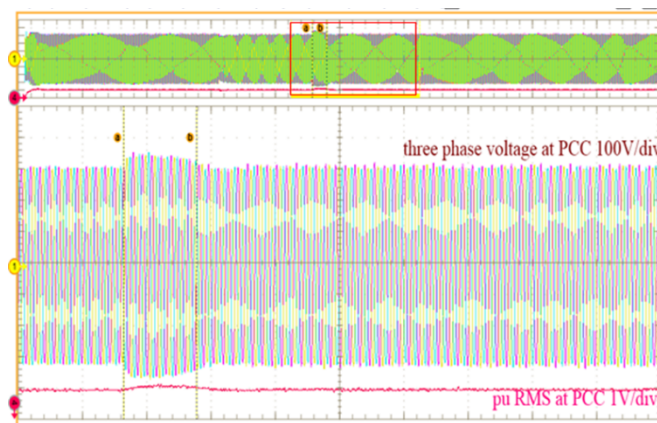


Fig. 16. RMS voltage and Instantaneous voltage at PCC ending of sag with DSTATCOM (Hardware in-loop)

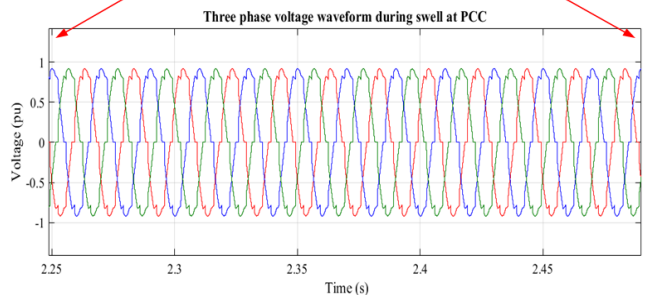


Fig. 19. RMS voltage and Instantaneous voltage at PCC with swell without DSTATCOM (Hardware in-loop)

1.1. Case VI:

In fig 20, voltage waveform at PCC with starting and ending of swell is shown. Previously to the swell, voltage was maintained at 1 pu. When swell occurs at 2 s, voltage starts to rise and controller takes 0.25 s to bring down voltage at 1 pu and finally the swell is cleared at 3 s. Fig 21 shows the voltage (RMS) at PCC and the real and reactive power supplied from DSTATCOM. The reactive power supplied from DSTATCOM is reduced when swell occurs

and voltage is maintained at 1 pu. Similar results are obtained in hardware in the loop simulation. Fig 22 and 23 show the three phase voltage waveform at the starting and ending of swell in hardware in the loop simulations.

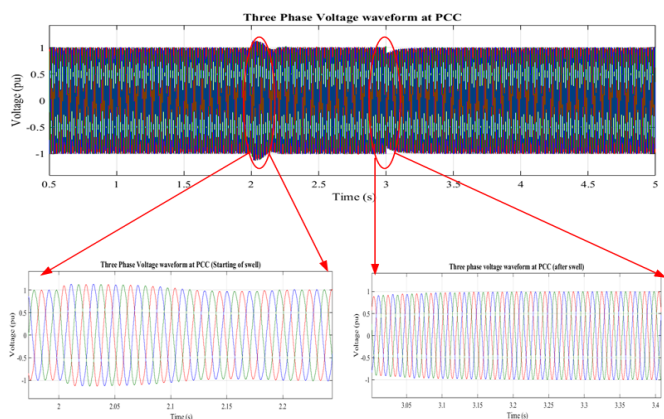


Fig. 20. Instantaneous voltage at PCC with DSTATCOM and with swell (MATLAB Simulation)

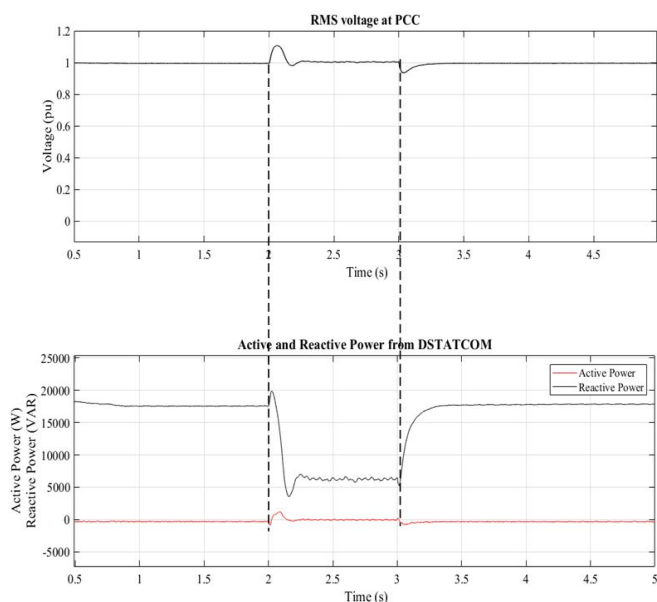


Fig. 21. RMS voltage at PCC with DSTATCOM with swell (MATLAB Simulation)

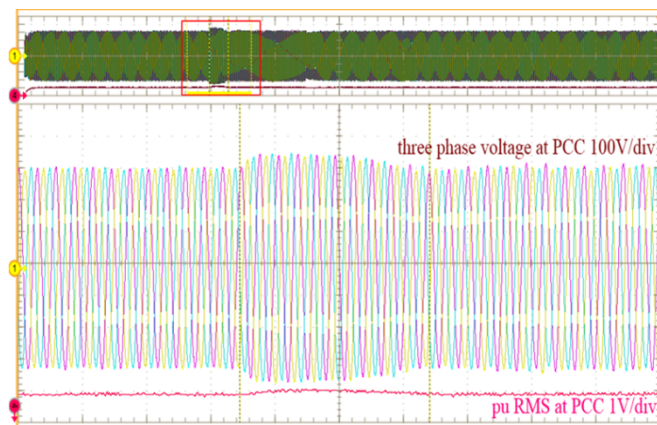


Fig. 22. RMS value of voltage and Instantaneous voltage at PCC starting of swell with DSTATCOM (Hardware in-loop)

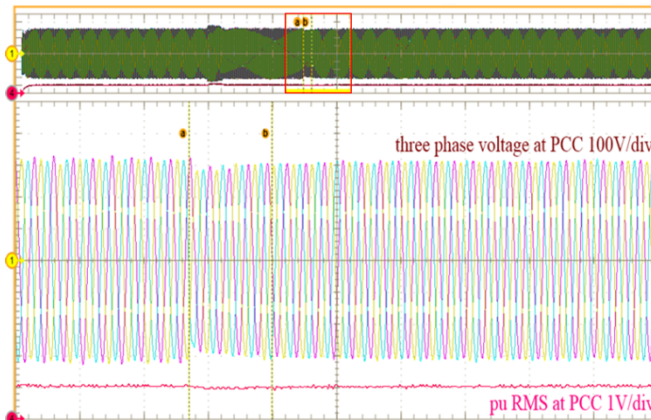


Fig. 23. RMS value of voltage and Instantaneous voltage at PCC ending of sag with DSTATCOM (Hardware in-loop)

From the results, it is observed that satisfactory operation of the controller works for the unbalanced and nonlinear load conditions. During the voltage disturbances i.e. swell and sag, the controller is able to maintain the voltage at the reference value, i.e. 1 pu. The reactive and active power supplied from the DSTATCOM is also observed. During the sag the reactive power supplied from the DSTATCOM is increased, whereas during swell reactive power supplied is reduced. Voltage is maintained at desired level in both the cases. The active power in both the cases are maintained at constant value.

4. Conclusion

In this paper, the current sensor-less controller is presented. The controller is simulated in MATLAB and is verified using hardware in loop simulation. It is observed that controller shows the satisfactory operation under nonlinear and unbalanced load conditions. The controller is also able to reduce the distortion in voltage waveform and sustain balance in voltage. During the voltage sag and swell conditions, the voltage is maintained within standard values by the improved controller.

Appendix

AC mains: 220 V (L-L), 50 Hz; Line impedance: 0.85 Ω , 2.25 mH; Unbalanced load: 60+j62.73 Ω , 40+j78.5 Ω , 50+j50.24 Ω ; Nonlinear load: Three phase uncontrolled rectifier with load of R= 25 Ω , L=0.01 H; C_{dc}: 800 μ F; R_f: 0.2 Ω ; L_f: 15 mH.

References

- [1] K. R. Devabalaji and K. Ravi, "Optimal size and siting of multiple DG and DSTATCOM in radial distribution system using Bacterial Foraging Optimization Algorithm", Ain Shams Eng. Journal, vol. 7, pp. 959-971, 2016.
- [2] N. G. Hingorani, "Introducing Custom Power", IEEE spectrum, pp. 41-48, June, 1995.

- [3] M. K. Mishra, A. Gosh, and A. Joshi, "Operation of a DSTATCOM in voltage control mode", IEEE Trans. Power del., vol. 18, NO. 1, pp. 258-264, January 2003.
- [4] C. Kumar and M. K. Mishra, "A Multifunctional DSTATCOM Operating Under Stiff Source," IEEE Trans. Industrial Electronics, Vol. 61, No.7, pp.3131-3136, 2014.
- [5] L. Comparatore, A. Renault, J. Pacher, J. Rodas and R. Gregor, "Finite Control Set Model Predictive Control Strategies for a Three-Phase Seven-level Cascade H-Bridge DSTATCOM", 7th International Conference on Renewable Energy Research and Applications, Paris, France, pp. 779-784, 14-17 October, 2018.
- [6] B. Singh, S.K. Dube and S. R. Arya, "An Improved Control Algorithm of DSTATCOM for Power Quality Improvement", Electrical Power and Energy Systems, vol. 64, pp. 493-504, 2015.
- [7] D. Amoozegar, "DSTATCOM Modelling for Voltage Stability with Fuzzy Logic PI Current Controller", Electrical Power and Energy Systems, vol. 76, pp. 129-135, 2016.
- [8] S. R. Arya and B. Singh, "Implementation of distribution static compensator for power quality enhancement using learning vector quantization," IET Generation, Transmission and Distribution, vol. 7, No. 11, pp.1244-1252, 2013.
- [9] S. R. Arya and B. Singh, "Performance of DSTATCOM Using Leaky LMS Control Algorithm," IEEE Journal of Emerging and Selected Topics in Power Electronics, Vol. 1, No. 2, pp.104-113, 2013.
- [10] S. R. Arya and B. Singh, "Neural Network Based Conductance Estimation Control Algorithm for Shunt Compensation," IEEE Trans. Industrial Informatics, vol. 10, No.1, pp.569-577, 2014.
- [11] B. Singh, P. Jayaprakash, S. Kumar, and D. P. Kothari, "Implementation of Neural-Network-Controlled Three-Leg VSC and a Transformer as Three-Phase Four Wire DSTATCOM," IEEE Trans. Industrial Applications, Vol. 47, No. 4, pp.1892-1901, 2011.
- [12] M. Mangaraj and A. K. Panda, "DSTATCOM Deploying CGBP based icos Φ neural network technique for power conditioning", Ain Shams Engineering Journal, 2016.
- [13] V K Kannan and N Rengarajan, "Photovoltaic based DSTATCOM for power quality improvement", Electrical Power and Energy Systems., Vol. 42, pp. 685-692, 2012.
- [14] C K Sundarabalan and K Selvi, "PEM fuel cell supported DSTATCOM for power quality enhancement in three phase four wire distribution system", International Journal of Hydrogen Energy, Vol. 39, pp. 19051-19066, 2014.
- [15] M. Thirupathiah, P. V. Prasad and V. Ganesh, "Enhancement of Power Quality in Wind Power Distribution System by using Hybrid PSO-Firefly based DSTATCOM", International Journal of Renewable Energy Research, Vol. 8, No. 2, pp. 1138-1154, 2018.
- [16] O.P. Mahela and A. G. Shaik, "Power Quality Improvement in Distribution Network using DSTATCOM with Battery Energy Storage System", Electrical Power and Energy Systems, vol. 83, pp. 229-240, 2016.
- [17] Kumar and M. K. Mishra, "A Voltage-Controlled DSTATCOM for Power-Quality," IEEE Trans. Power Delivery, Vol. 29, No.3, pp.1499-1507, 2014.
- [18] Kumar and M. K. Mishra, "An Improved Hybrid DSTATCOM Topology to Compensate Reactive and Nonlinear Loads," IEEE Trans. Industrial Electronics, Vol. 61, No. 12, pp.6517-6527, 2014.
- [19] W. Chen, and Y. Hsu, "Direct Output Voltage Control of a Static Synchronous Compensator Using Current Sensorless," IEEE PES Transmission and Distribution Conference and Exposition, Vol 3, pp. 545-549, 2003.
- [20] Y Zhang and J V Milanovic, "Global voltage sag mitigation with facts-based devices," IEEE Trans. Power Delivery, Vol. 25, No. 4, pp:2842-2850, 2010.
- [21] Ghosh and G. Ledwich, "Power quality enhancement using custom power devices," The Kluwer International Series In Engineering and Computer Science, Springer Science Buisness Media, LLC.
- [22] K R Padiyar, "FACTS controllers in power transmission and Distribution," New Age International Publishers.
- [23] IEEE Standard 519-1992, Recommended practices and requirements for harmonic control in electrical power systems, The Institute of Electrical and Electronics Engineers, 1993.